

# Thermal Stress Analysis in Structural Elements of HRSG Casing

Hyuntae Shin<sup>1</sup>, Daehee Kim<sup>2</sup>, Hyungjun Ahn<sup>2</sup>, Sangmin Choi<sup>2,\*</sup>, Gichul Myoung<sup>3</sup>

<sup>1</sup>Power Plant Engineering Dep., Samsung Engineering Co., Ltd., Seoul, 135-708, South Korea

<sup>2</sup>School of Mechanical Aerospace & Systems Engineering, Korea Advanced Institute of Science and Technology, Daejeon, 305-701, South Korea

<sup>3</sup>R & D Center, SeenTec Co., Ltd., Changwon, 641-969, South Korea

**Abstract** Heat recovery steam generators (HRSGs) are arranged at the tail end of gas turbines in combined cycle power plants (CCPPs), and are designed to withstand the hot gas environment approaching 600°C. In addition to higher thermal to power efficiency, CCPPs show superior response characteristics compared to those of other conventional steam power plants. For that reason, frequent load changes on the system, which sometimes include daily start and stop (DSS) operation, would impose additional burden on the structural elements. The main objective of this work is to analyze the thermal stress conditions as related to the observed failure on the structural elements of HRSG casing, and to find root causes of failure of mechanical integrity. To achieve this goal, field measurements were performed to record temperatures of wall and stiffener of the casing from a real plant in operation. To consider the effect of hot gas on the casing, computational fluid dynamic (CFD) analysis of gas flow inside the HRSG with appropriate wall conditions using FLUENT V12. Thermal stress analysis on the thin wall of the casing and stiffeners of HRSG was conducted with the temperature data from the CFD results, using ANSYS Workbench V12. Summarizing the computational results, some limited ideas were presented which would be useful to prevent damages.

**Keywords** Heat Recovery Steam Generator, Thermal Stress, Casing, Finite Element Analysis, Computational Fluid Dynamics

## 1. Introduction

Combined cycle power plants (CCPPs) enhance power generating efficiency by utilizing waste heat from the gas turbines, which would dispense some 60% of fuel energy as exhaust heat[1]. Waste heat is recovered to produce steam to generate electricity through a steam turbine. As a result, net thermal to power efficiency could exceed 50% in modern CCPPs[2](see Table 1). Heat recovery steam generator (HRSG) is a kind of a heat exchanger (or a boiler), which is connected to exit side of gas turbine(s). In general, exhaust gas from the gas turbine is cooled from 600°C to 100°C, while water is superheated to 540°C (at 12 MPa), in one of the typical plants (see Figure 1). Gas to water-steam heat exchangers are typically of finned tube type, and multiple layers of heat exchanger tube banks are stacked in a container, whose integral part is called HRSG. Because pressure of the gas is almost atmospheric and temperature of the gas is not high enough to require radiative furnace surface, walls of the HRSGs are simply a casing with

moderate thermal insulation. Selection of casing material and insulation must accommodate the service requirements in the hot gas environment.

**Table 1.** Typical modern day combined cycle performance[2]

Combined cycle performance	% of fuel heat input
Fuel input LHV	100
Gas turbine power	36
Gas turbine losses	1
Gas turbine exhaust heat	63
Stack loss	22
Input to steam	41
Steam losses	1
Steam power	19
Heat to condenser	21
Gross electric power	55
Auxiliaries power	2
Total net power & efficiency	53

Besides the higher thermal efficiency, gas turbine combined cycle power plants are typically characterized by their flexibility, quick part-load starting, being suitable for both base-load and cyclic operation. Usually, it takes 3 hours to reach the full load operation after 8 hour's shut down for the fossil fired steam plants of 500MW scale, but it takes only 1 hour for CCPPs[3]. Hence, many CCPPs are installed to manage peak and cyclical loads and are running

\* Corresponding author:

smchoi@kaist.ac.kr (Sangmin Choi)

Published online at <http://journal.sapub.org/ijee>

Copyright © 2012 Scientific & Academic Publishing. All Rights Reserved

on the daily start and stop (DSS) operation mode. Repeated incidents of transient conditions, when all operating parameters including temperature, pressure and mass flow show rapid change, should be considered in addition to the steady-state thermal design environment.

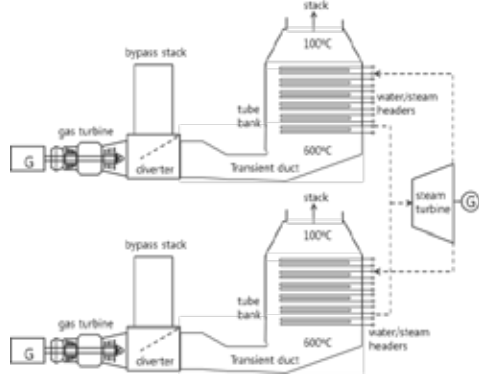


Figure 1. A schematic of a HRSG in a typical CCP

HRSG components are subject to high thermal stress, and the drum and headers are vulnerable to stress[4], which include thermal and mechanical stresses. Thermal stress is caused by temperature difference of the service environment, and mechanical stress is caused by the steam pressure. From the previous studies[5, 6], it was shown that a bias in the flow of a HRSG would lead to the temperature and stress imbalance on tubes, and it can be a cause of damage on tubes. When the integral plant units including gas turbine and HRSG experience dynamic load conditions, more serious is its effect on shortening the service life[7]. In connection with this problem, considerable studies have been carried out to analyze and improve dynamic conditions of start-up process[7-11]. Also, the casing of HRSG can be easy to damage during the start-up. However, researches related with these problems have not been conducted as much as the gas turbine or steam turbine casings which have the same cases of failure[12-15].

Objective of this study is to find remedy to the observed failure of the structural elements of HRSG casing through the understanding of thermal stress behaviors of the HRSG casing during the system operation. Field measurements of casing wall temperature were performed during the start-up phase of the plant in commercial operation, in addition to the hot steady state condition. To elucidate the effect of hot gas flow state on the casing wall, computational fluid dynamic (CFD) analysis were carried out and the results were directly used as input conditions of finite element method (FEM) stress analysis model. Based on the stress analysis results, some limited ideas were proposed which would prevent the casing damages.

## 2. HRSG Plant: Observation and Measurements

### 2.1. Plant Description

Figure 1 shows the general arrangement of the HRSG of the plant considered in the case, which has 2x150MWe gas turbines and one 190MWe steam turbine. Each of the gas turbine is connected to its corresponding HRSG, and steam lines from two HRSGs are connected to a single steam turbine. Inside of HRSG, gas side temperature and pressure would drop as the gas flows across the tube banks. Tube banks of the HRSG are covered by a casing and stiffeners to support a thin-wall casing as shown in Figure 2. The entire HRSG is roughly divided into 3 parts as upper, middle and bottom, whose division is also roughly corresponding to the gas temperature and the mean temperature of the heat exchanger tube banks. Because of this temperature difference, different type of casing material and insulation are used in each part. Table 2 shows the selected casing material and insulation conditions of the designated casing wall. Inner insulation is only used in the bottom section to protect the duct plate from the relatively high gas temperature. Detailed view of the arrangement of the casing and insulation in the bottom section is shown in Figure 3. 6mm casing plate (duct plate) is covered by insulation blankets (inside 100mm, outside 300mm). The casing is also supported by outside stiffeners, type 1 and type 2.

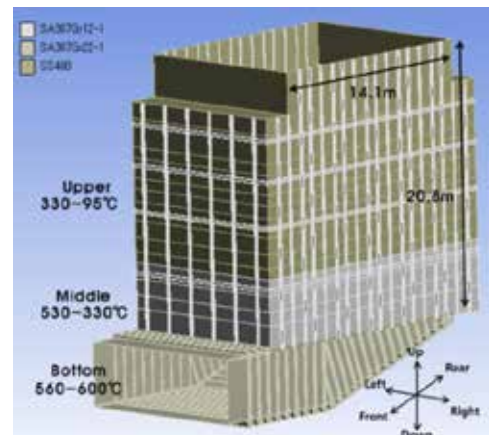


Figure 2. HRSG casing wall and stiffener arrangement

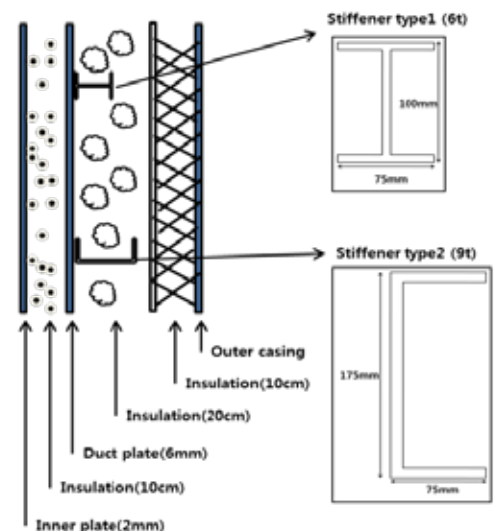


Figure 3. HRSG casing wall and stiffener arrangement

**Table 2.** Casing materials and insulation condition

	Section		
	Upper	Middle	Bottom
Gas temp. (°C)	95~330	330~560	560~600
Casing material	SS400	SA387Gr12-1	SA387Gr22-1
Insulation material (blanket)	Mineral	Ceramic/Mineral	Ceramic/Mineral
Thickness of insulation	Outer 200 mm	Outer 200 mm	Inner 100 mm Outer 200 mm

Power plants are expected to run on the full load conditions, which is roughly corresponding to the most severe design condition. However, CCCPs typically experience frequent load changes including start-up from dead state. On average, a CCPP will go through 50 cold, 80 warm and 200 hot starts, each year: in cold starts, more than 48 hours has passed since the last synchronization of the gas turbine, hot starts less than 8 hours, and warm starts in between. In the current case of CCPP, it takes 240 minutes for the cold start-up, 80 minutes for the warm start-up and 60 minutes for hot start-up. It is expected that the most severe design point as related to the strength of material should be based on the steady state full load condition with a reasonable design margin, while repetition of start-up and cool-down should be considered for the fatigue-based failure analysis.

## 2.2. Observed Failure in Structural Elements

There have been several reports of damage on casing and tubes in the HRSG, which include broken casing, snapped stiffeners and elongated fin tubes. Some example photographs, which were taken after 7 years of commercial operation, are shown in Figure 4, (a) snapped stiffener and (b) broken casing.

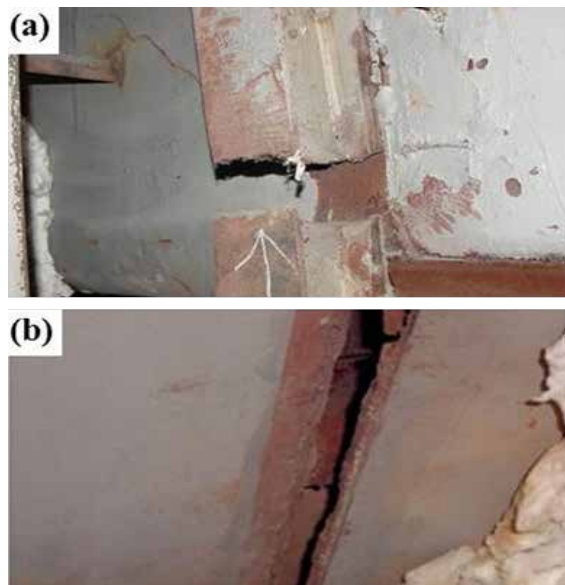


**Figure 4.** Photographs of damaged part on HRSG: (a) Snapped stiffeners, (b) Broken casing

## 2.3. Field Measurements

In an attempt to quantitatively determine the thermal response of the HRSG casing, temperatures at selected

positions on the casing and stiffeners were measured. K-type thermocouples were welded on the casing wall plates and stiffener beams, and data were collected by Yokogawa MV2048 multi-recorder. Total 14 points on the bottom casing and stiffeners were selected; 3 points on the side wall and 4 points on the rear wall as shown in Figure 5. Collected measurement data were compiled along with the necessary information from the existing data logging system of the plant.

Gas-side temperature would be changing depending on the gas turbine load conditions among others, and temperature of HRSG casing walls would also be affected by heat transfer from the gas flow as well as heat loss to the environment. The questions related with temperature would include the absolute value of (for example, highest) temperature and time response of temperature at the selected positions. Two sets of measurement campaign were designed to derive information; time-wise recording of the temperature measurements at the selected positions during a cold start-up and a hot start-up. During the cold start-up, wall temperatures will rise from atmospheric, while the whole plant is being warmed-up through a relatively long transient process. The hot start-up case will provide information of the steady state value after passing through a short transient period.

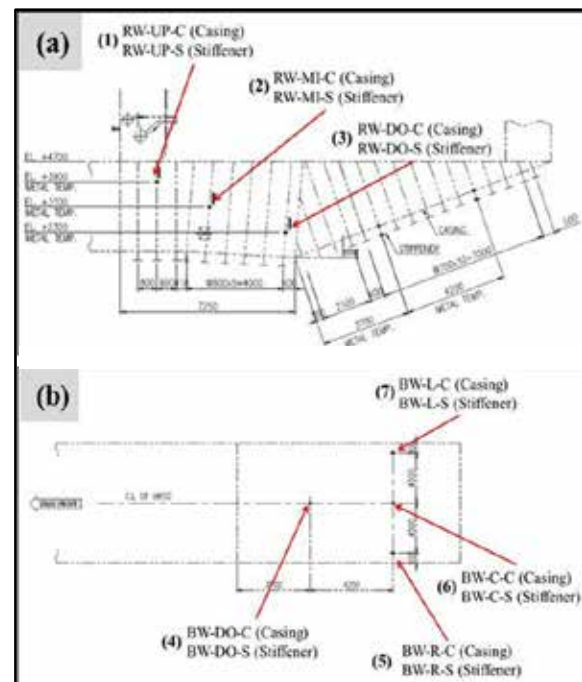


**Figure 5.** Temperature measurement points for wall and stiffener: (a) Side wall, (b) Rear wall

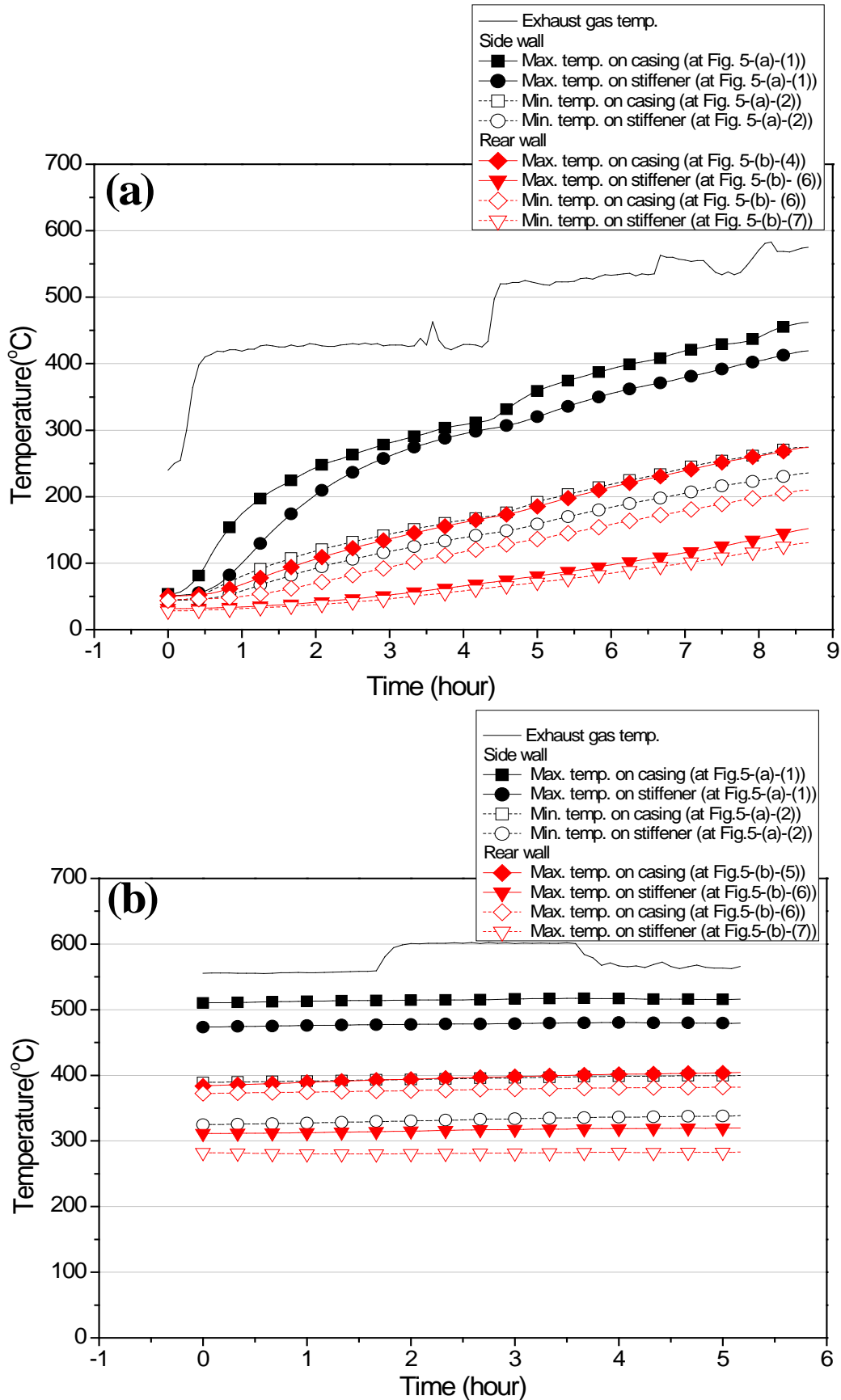


Figure 6. Temperature measurement data: (a) Cold start and load following, (b) Hot start and load following

The first measurement campaign was performed to observe the heat-up process of the plant during the cold start-up, until the gas turbine reached the full load. This was a rather slower ramping which took some 8 hours. The results are shown in Figure 6-(a). The casing and stiffener temperature in the side wall and rear wall were expressed at maximum and minimum value among measured temperature sets. Gas temperature during the warm-up period remained almost constant at 430°C, and increased to over than 530°C and was fluctuating as the plant power output was following the load requirement of the grid system. A typical set of wall temperatures on the casing wall and on the stiffener are shown in the figure. The wall temperatures did not reach their corresponding steady state value, and kept rising even after 8 hours after cold start. Casing wall and stiffener temperatures are strongly dependent on the location of the measurement. Especially, casing and stiffener temperature in the upper part of side wall (Figure 5-(a)-(1)) have maximum value and those are affected by gas turbine load change more severely as compared to other points. From this, we could estimate the casing damage and thus gas leakage in this part. Stiffener temperatures are typically lower than casing by some 40°C at the side wall and 100°C at the rear wall, which represents the conductive thermal resistance.

The second set of measurements (during a warm start-up with 2-hour fixed-load operation) was performed to identify the highest temperature on the casing, and the results are shown in Figure 6-(b). Gas temperature basically represents the load condition of the turbine, where 2-hour peak-shaving operation mode is shown. Casing wall and stiffener temperatures are still strongly dependent on the location of the measurement, but those do not show noticeable difference according to time, which means that the plant is almost uncooled during the stand-by period. The temperatures are believed to represent typical operating condition of the hot plant.

### 3. Computational Analysis of Gas-side Flow, Heat Transfer and Thermal Stress in Casing Structure

#### 3.1. Approach

Hot gas flow from the gas turbine is introduced into the HRSG through a transition duct. It is of our interest to understand thermal stress in the structural elements of HRSG casing. Analysis of thermal stress would require comprehensive information of local temperature of structural elements. Field measurements of temperature on the selected positions could not provide adequate data for stress analysis, so combined simulation of gas-side flow and heat transfer and thermal stress in casing structure was performed. Geometric information is based on the unit considered in this case, and operating conditions information which is based on 100% full load operation are

summarized in Table 3. Input values to express the pressure and temperature drop at the tube zone were decided based on data of the pressure and temperature in the Ulsan combined cycle power plant unit 2 as shown in Table 4. Both of the fluid dynamics and stress analysis are based on the steady state operation. Wall temperature data calculated from the CFD simulation was used for input condition in stress analysis.

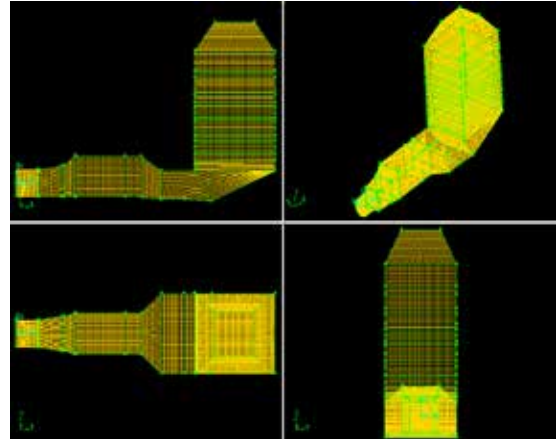


Figure 7. Measured temperature profile of exhaust gas, superheater tube wall and steam

Table 3. Inlet condition [16]

	Value	
Flow rate	345	
Temp. of exhaust gas (°C)	605	
Exhaust gas composition (% weight, ambient temp. 15°C)	O <sub>2</sub>	14.5
	CO <sub>2</sub>	5.7
	H <sub>2</sub> O	5.0
	N <sub>2</sub>	73.5
	Ar	1.3

Table 4. Pressure and temperature change at each level in tube zone [16]

Level of tube bank	Δ Pressure (Pa)	Δ Temperature (K)
1	290	81.5
2	550	183
3	410	59
4	200	28
5	320	52
6	430	52
7	400	49

#### 3.2. CFD Model

The computation domain starts from the tail end of gas turbine and extends to the exit of the HRSG connected to the stack (see Figure 7), to investigate the effect of geometry of the duct. One can notice that the main and by-pass stacks of HRSG were excluded from the domain. The grid pattern was selected in such a manner that the grid spacing was sufficiently fine for the region near the entrance of the tube zone. The total volume was divided into approximately 3 million elements. Fluent V12 was used for the numerical simulation with the RNG  $k-\epsilon$  turbulence model [17]. Simulation of the tube zone was made possible by adopting a porous media assumption. Pressure drop across the tube banks was

calculated as a source term added in momentum equation[18]. Number of Transfer Unit (NTU) model was used to calculate the heat transfer in the tube zone. Fan swirl velocity modelling was employed to express the swirl flow from the gas turbine[19]. Heat transfer from the hot gas to the wall is described by convective heat transfer. The convective heat transfer coefficient was calculated from the equation of turbulent duct heat transfer (Eg. (1))[20], which is different from the common correlation for turbulent flow, under the assumption that the thermal-flow in the boiler is like a duct flow.

$$Nu_d = \frac{hd}{k} = 0.069 Re_d^{0.8} Pr^{0.4} \quad (1)$$

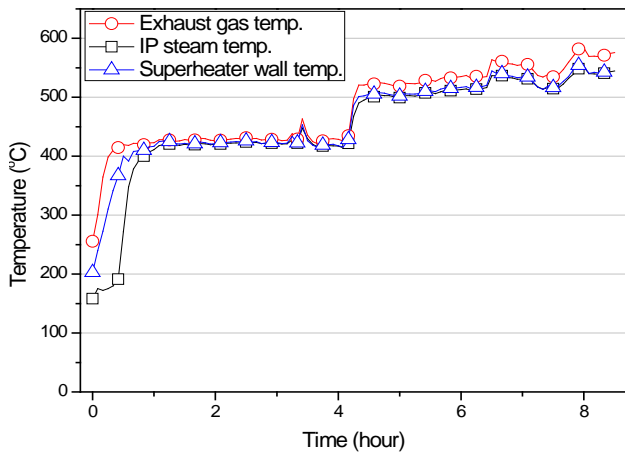


Figure 8. Measured temperature profile of exhaust gas, superheater tube wall and steam

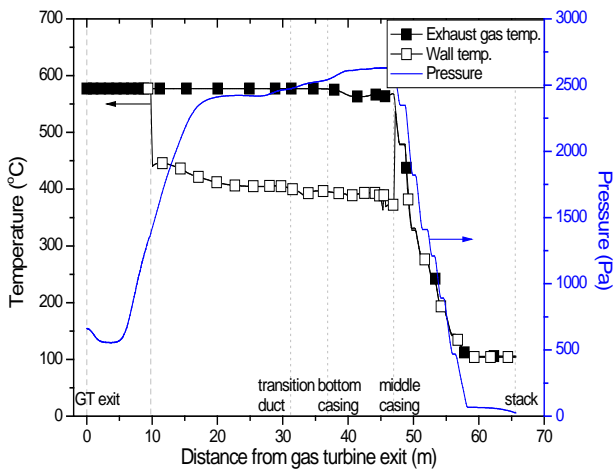


Figure 9. Computed mean free stream temperature, wall temperature, and static pressure along the gas flow path(GT exit to stack)

In middle and upper sections, the wall temperature was assumed to be same as the gas temperature by setting wall adiabatic condition. Figure 8 presents the measured temperatures of super-heater tube wall, exhaust gas and steam in tube. About 1 hour later, all temperatures had same behavior, so wall which has no inner insulation would show the same behavior with the gas temperature too.

Casing walls are insulated internally and/or externally. To verify the proposed heat transfer relations, computed

temperature at selected positions were compared with measurements data. Also, the temperature and pressure drop across the HRSG tube banks were compared between the measurements and computation. These were considered as additional validation of the approach.

### 3.3. CFD Result

Figure 9 shows exhaust gas temperature, wall temperature and pressure profile along the gas flow path ranging from the gas turbine exit to the stack by CFD analysis. Gas turbine exhaust gas temperature, which is approximately 580°C, is almost constant to the middle casing section. However, wall temperature decreases to 440°C at 9.8m from the gas turbine exit and decreases gradually to 370°C before the middle casing section. This wall temperature decrease is because of the boundary condition setting as no inner insulation. At the middle casing part, which has inner insulation, the casing temperature increased sharply. This sharp temperature increase is because that conduction heat transfer between adjacent casings is not considered in this CFD analysis. As expected, with passing each tube zone, both wall temperature and pressure decreased from 567°C , 2.6MPa to 100°C , 26Pa as a result of gas temperature decrease by heat exchange. Each seven horizontal short line in wall temperature and pressure from the middle casing to the stack means the heat exchange between hot gas and water in the tube zone. In the tube zone section, wall temperature is the same as gas temperature as a result of our analysis setting as explained in the previous section. These CFD results match well with the wall temperature and pressure of tube zone in the operation data of Ulsan combined cycle power plant unit 2 as shown in Figure 10.

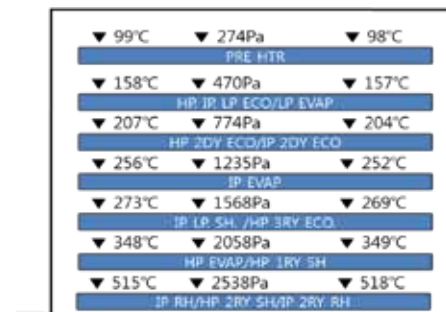


Figure 10. Operation data[16]

### 3.4. Thermal Stress Analysis

Finite element stress analysis was conducted using ANSYS workbench V.12[21]. General boilers are supported by a hot beam at the top of the casing to consider heat expansion during operation, and this situation is the same at HRSGs. So fixed support condition at the top of the HRSG model was used. To conduct thermal stress analysis, wall temperature data from the CFD simulation was imported

into the FEM model. The stiffener temperature was set reasonably as 144°C at the maximum load of gas turbine (cold start-up case) and 300°C at the steady state (hot start-up case) from the measured data on the rear wall. Wall pressure information from the CFD simulation was also used as input data for thermal stress analysis and it is shown in Figure 9. The wall pressure was about 2.6MPa at the middle casing and kept decreasing about 26Pa until the inlet to the stack.

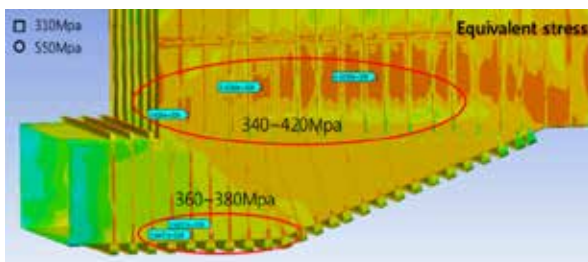
### 3.5. Results and Interpretation

Figure 11 and Figure 12 show the results of stress analysis at full load of gas turbine (cold start-up case) and at steady state (hot start-up case). In figures, the stress over the minimum yield stress suggested by ASME Boiler & Pressure Vessel Code was presented as a square box and the stresses over the yield stress suggested by Ahn *et al.* was presented as a circle box. Those values are 310MPa and 550MPa [22,23].

At the full load of gas turbine in cold start-up case, maximum stress appeared in the middle casing part of side wall and in the front stiffener of bottom section as shown in Figure 11. At the steady state analysis in hot start-up case, maximum stress appeared in the same position with the full load case, but the value decreased as shown in Figure 12. The values of the maximum stress in two cases are summarized in Table 5. At the time of full load of gas turbine, on stiffener, the stress range on concentrated area was calculated as 360~380MPa and these stress values are over the minimum yield stress suggested by the Code, 310MPa. So the damage as shown in Figure 4-(a) arose at this area actually. On the side wall, the maximum stress range was calculated as 340~420MPa and the casing failure could be expected on this area, where is the boundary area between the inner insulation and none the inner insulation zone. According to the previous temperature measurement, much higher casing temperature compared to the others appeared near this concentrated stress area. So it might be that the leaked hot exhaust gas from this broken casing increased the casing temperature.

**Table 5.** Equivalent stress at stress concentration area of each case

Case	Casing wall stress (MPa)	Stiffener stress (MPa)
Full load of GT	340~420	360~380
Steady state	180~360	310~350



**Figure 11.** Result of thermal stress analysis at full load of gas turbine (cold start-up case) (a square box: the stress over the minimum yield stress suggested by ASME Boiler & Pressure Vessel Code, a circle box: the

stresses over the yield stress suggested by Ahn *et al.*)

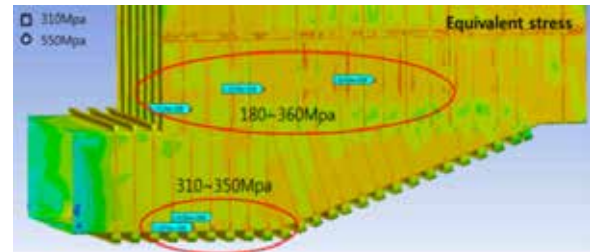


**Figure 12.** Result of thermal stress analysis at steady state (hot start-up case) (a square box: the stress over the minimum yield stress suggested by ASME Boiler & Pressure Vessel Code, a circle box: the stresses over the yield stress suggested by Ahn *et al.*)

When the wall temperature reached to peak and steady state, the stress occurring on the side wall was mitigated as compared to the case of full load of gas turbine and the values were less than 310MPa except only little area. This thermal stress decrease is because a big difference of adjacent casing temperature between inner insulation and none inner insulation zone during cold start-up was mitigated with changing to the steady state of hot start-up case. However, the stresses on stiffeners were still high as 310~350MPa, which are over the minimum yield stress value.

From this result, the insulation configuration and its location on casing should be carefully selected to prevent large thermal stress by temperature difference of adjacent casing during start-up. Furthermore, the fixed constraint between wall and stiffener considered in the present analysis is not enough to endure thermal expansion and other method, such as sliding constraint should be considered.

## 4. Conclusions

In this study, field measurements and combined fluid flow and thermal stress analysis were carried out to understand repeated thermal loading and its behavior on the HRSG casing during the start up. Analysis were conducted at two moments, when gas turbine reached to full load and wall temperature increased to its corresponding peak and steady state. From the present study, following conclusions can be drawn:

1. During the start-up, stress concentration occurred at boundary between the wall with inner insulation and the other one without inner insulation. The values were over the minimum yield stress suggested. Also, high stress concentration appeared on the stiffener, where physical destruction was observed.

2. When the wall temperature reached to the peak and steady state, high temperature gradient on the side wall decreased and stress was mitigated as well. However, stresses on the stiffeners were still high. Repeated thermal loading on that area might be a main reason of casing failure.

3. To prevent damage on HRSG casing and stiffener, the

insulation configuration and its location on casing should be carefully selected to prevent arising large temperature difference and thus large thermal stress. Moreover, the constraint between wall and stiffener, such as sliding must be considered to solve the thermal expansion problem presented in this fixed constraint.

## ACKNOWLEDGEMENTS

The present work was supported by SeenTec Co. Ltd. and Brain Korea 21.

## REFERENCES

- [1] J. H. Horlock, *Combined Power Plants including Combined Cycle Gas Turbine (CCGT)*, Pergamon Press, Oxford, 1992
- [2] *Technology Status Report: Heat Recovery Steam Generator Technologies*, Cleaner Coal Technology Programme, 2003
- [3] K. G. Choi, *A Study on the Variations of Duct Inside Turbulent Flow Structure and Heat Transfer Characteristics by Transition Duct Configuration*, Ph. D. Thesis, Changwon University, Changwon, Republic of Korea, 2008
- [4] Kim, T. S., Lee, D. K., and Ro, S. T., 1999, Analysis of thermal stress evolution in the steam drum during start-up of a heat recovery steam generator, *Applied Thermal Engineering*, 20, 977~992
- [5] Tenbusch, A. F., 2003, CFD modeling of cogeneration burner applications and the significance of thermal radiative heat transfer effects, *Proceeding of International Joint Power Generation Conference*, 731-742
- [6] Shin, H. T., Kim, D. H., Ahn, H. J., Choi, S. M., and Myoung, G. C., 2012, Investigation of the flow pattern in a complex inlet duct of a heat recovery steam generator, *Energy and Power*, 2(1), 1-8
- [7] Matsumoto, H., Takahashi, S., Akiyama, T., and Ishiguro, O., 1996, An expert system for startup optimization of combined cycle power plants under NOx emission regulation and machine life management, *IEEE Transactions on Energy Conversion*, 11(2), 414~422
- [8] Kim, T. S., Lee, D. K., and Ro, S. T., 2000, Dynamic behavior analysis of a heat recovery steam generator during start-up, *International Journal of Energy Research*, 24(2), 137~149
- [9] Shin, J. Y., Jeon, Y. J., Maeng, D. J., Kim, J. S., and Ro, S. T., 2002, Analysis of dynamic characteristics of a combined-cycle power plant, *Energy*, 27 (12), 1085~1098
- [10] Shirakawa, M., Nakamoto, M., and Hosaka, S., 2005, Dynamic simulation and optimization of start-up processes in combined cycle power plants, *Japan Society of Mechanical Engineering International Journal*, 48(1), 122~128
- [11] Alobaid, F., Postler, R., Strohle, J., Eppe, B., and Kim, H. G., 2008, Modeling and investigation start-up procedures of a combined cycle power plant, *Applied Energy*, 85(12), 1173~1189
- [12] Mustaga, A. H., Hashmi, M. S., Yilbas, B. S., and Sunar, M., 2008, Investigation into thermal stresses in gas turbine transition-piece: Influence of material properties on stress levels, *Journal of Materials Processing Technology*, 201(1-3), 369~373
- [13] Kang, M. S., Yun, W. N., and Kim, J. S., 2009, Investigation of the thermo-mechanical crack initiation of the gas turbine casing using finite element analysis, *The Korean Society for Power System Engineering*, 13(5), 52~58
- [14] Lee, B. Y., and Cho, J. R., 1998, Structural analysis of high pressure steam turbine casings for power plants using the BEM and the FEM, *The Korea Society of Marine Engineering*, 22(5), 609~616
- [15] Choi, W., and Hyun, J., 2008, A life assessment for steam turbine casing using inelastic analysis, *Modern Physics Letters B*, 22(11), 1141~1146
- [16] *Data Book of Ulsan Combined Cycle Power Plant Unit 2*, Korea Power Engineering Company Inc., 1997
- [17] *Fluent 6.3 User's Guide*, FLUENT Inc., 2006
- [18] Cho, J. M., Choi, J. W., Hong, S. H., Kim, K. C., Na, J. H., and Lee, J. Y., 2006, Application of computational fluid dynamics analysis for improving performance of commercial scale selective catalytic reduction, *Korean Journal of Chemical Engineering*, 23(1), 43~56
- [19] Yoo, G. J., Choi, H. K., Choi, K. L., and Shin, B. J., 2009, A numerical study of the turbulent flow characteristics in the inlet transition square duct based on roof configuration, *Transaction of Korea Society of Mechanical Engineers(B)*, 33(7), 541~551
- [20] F. R. Steward, *Mathematical Simulation of Industrial Boiler by the Zone Method of Analysis*, Heat transfer in Flames, Scripta Book Company, 1974
- [21] S. Moaveni, *Finite Element Analysis – Theory and Application with ANSYS*, Pearson Education, 2008
- [22] *ASME Boiler & Pressure Vessel Code Sec. II*, ASME, 2007
- [23] Ahn, S. G., Huh, Y. H., and Park, J. H., 2000, Measurement and application of J-R curves of Cr-Mo steel and Cr steel, *Transaction of Korea Society of Mechanical Engineers(A)*, 328~332